ELSEVIER

Polymer 41 (2000) 3205–3211

polymer

Poly(styrene-*b*-isobutylene-*b*-styrene) block copolymers and ionomers therefrom: morphology as determined by small-angle X-ray scattering and transmission electron microscopy

R.F. Storey*, D.W. Baugh III[1]

Department of Polymer Science, The University of Southern Mississippi, Box 10076, Hattiesburg, MS 39406-0076, USA

Received 3 September 1998; received in revised form 13 July 1999; accepted 15 July 1999

Abstract

Solvent-cast films of poly(styrene-*b*-isobutylene-*b*-styrene) (PS–PIB–PS) block copolymers and block ionomers were analyzed using small-angle X-ray scattering (SAXS) and transmission electron microscopy (TEM). Four block copolymer samples with center block molecular weights of 52,000 g mol^{-1} and PS volume fractions (ϕ_{PS}) ranging from 0.17 to 0.31 were studied. Block ionomers were produced by lightly sulfonating the PS outer blocks of the PS–PIB–PS block copolymers. Sulfonation levels were 1.5 and 3.4 mol%, and sodium and potassium counterions were studied. All samples exhibited hexagonally packed cylinders of PS within the PIB matrix. Cylinder spacing was in the range 32–36 nm for most samples, while cylinder diameters varied from 14 to 21 nm. Porod analysis of the scattering data indicated the presence of isolated phase mixing and sharp phase boundaries. © 2000 Elsevier Science Ltd. All rights reserved.

Keywords: Poly(styrene-*b*-isobutylene-*b*-styrene) block copolymers; Morphology; Porod analysis

1. Introduction

Triblock copolymers of the A–B–A type, which phase separate due to thermodynamic immiscibility of the constituent blocks, are the subject of widespread interest due to their unique morphologies and useful properties. Of special interest are the so-called thermoplastic elastomers (TPEs) which are composed of glassy outer blocks and rubbery inner blocks. Phase separation of the glassy blocks into discrete domains results in materials that behave as crosslinked rubbers at low temperatures, but can be processed as thermoplastics at higher temperatures. The glassy domains, typically polystyrene (PS), act as reinforcing filler and provide physical crosslinks which can be weakened by heating to temperatures above their T_g.

Recently, triblock copolymers based on polyisobutylene (PIB) inner blocks and PS outer blocks have become available through the process of controlled/living cationic polymerization [1–6].[2] The fully saturated rubbery block confers excellent thermal and oxidative stability to these materials, and it enables certain post-polymerization modification reactions to be carried out exclusively within the PS segments. For example, Storey et al.[7] produced PIB-based block copolymer ionomers by lightly sulfonating the PS blocks of PS–PIB–PS triblock copolymers, thereby introducing additional physical crosslinks in the form of ionic aggregates. These ionic crosslinks remain stable up to much higher temperatures, resulting in improved modulus at temperatures above the T_g of PS.

The morphology of A–B–A block copolymers, i.e. the size, shape, and spatial arrangement of the phase-separated domains, depends primarily on the relative volume fractions of the two components, the difference in their solubility parameters, sample preparation and thermal history [8,9]. For a given block copolymer system, it is important to understand and control the parameters that affect morphology since the latter strongly affects mechanical properties. Inclusion of ionic groups into the hard domains is an additional complicating factor. Weiss and coworkers [10–13] studied poly(styrene-*b*-ethylene-*co*-1-butene-*b*-styrene) (SEBS)-based block copolymer ionomers at various sulfonation levels using solution cast and compression molded films. These authors postulated that light sulfonation of the PS blocks introduces two competing effects that may affect morphology, and hence mechanical properties of the system

---

* Corresponding author. Tel.: +1-601-266-4868; fax: +1-601-266-5504. *E-mail address:* rstorey@www.psrc.usm.edu (R.F. Storey).

[1] Present address: The Dow Chemical Company, Freeport, TX 77541, USA.

[2] PIB-based thermoplastic rubbers are available commercially from Kuraray Co., Ltd., 41, Miyukigaoka, Tsukuba City, Ibaraki Prefecture 305, Japan.

0032-3861/00/$ - see front matter © 2000 Elsevier Science Ltd. All rights reserved.
PII: S0032-3861(99)00512-1

Table 1
PS–PIB–PS block copolymer compositions determined by NMR and GPC

Sample	$M_{p,PIB}$ (g mol^{-1} × 10^{-3})	MWD_{PIB}	ϕ_{PS}	$w_{PS,NMR}$	M_{PS} [a] (g mol^{-1} × 10^{-3})	$MWD_{PS-PIB-PS}$
BCP04	51.9	1.09	0.172	0.192	6.2	1.33
BCP01	53.0	1.17	0.231	0.255	9.1	1.48
8907	51.8	1.16	0.296	0.324	12.4	1.41
BCP02	51.7	1.07	0.308	0.337	13.1	1.43

[a] PS block molecular weights calculated from NMR and GPC data as described in Section 2.

[10]. The ionic groups attached to the PS chains are expected to result in a greater driving force for phase separation due to the increased difference in solubility parameters of the constituent blocks, but phase separation may be impeded by the reduced mobility of the ionomer blocks. The result of these competing effects is not completely understood.

In a three-part series of papers [14], we have rigorously investigated the composition, morphology and properties of several PS–PIB–PS triblock copolymers, and ionomers derived therefrom, possessing similar PIB center blocks and PS outer blocks of varying sizes. This, the second paper of the series, focuses on the morphological investigation of the materials using small-angle X-ray scattering (SAXS) and transmission electron microscopy (TEM). Special attention was given to the preparation of solution cast films of both the hydrocarbon block copolymers and the ionomers. This resulted in ionomer films with well-developed phase morphology. In this paper, we present the first TEM micrographs of a block copolymer ionomer showing hexagonally packed, cylindrical PS ionomer domains with excellent long-range order, as well as supporting SAXS data displaying more clearly defined higher order peaks than that have been shown in previous studies of similar block copolymer ionomers [10].

2. Experimental

2.1. Materials

Linear PS–PIB–PS block copolymers were synthesized using a 1,3-di(2-chloro-2-propyl)-5-*tert*-butylbenzene/$TiCl_4$ initiating system employing pyridine as an externally added electron donor and di-*tert*-butyl pyridine (DTBP) as a proton trap in 60/40 (v/v) hexane/methyl chloride cosolvents at −80°C; details of the block copolymer synthesis have been previously reported in Part I of this three-part series of papers [14]. Compositions of block copolymers, summarized in Table 1, were determined using proton nuclear magnetic resonance (NMR) and gel permeation chromatography (GPC) as described below.

Proton NMR was used to determine block copolymer composition (weight fraction PS, $w_{PS,NMR}$) by comparing the integrated areas of the aromatic (6–8 ppm) and aliphatic (0.5–2.5 ppm) regions of the spectra, denoted A_{arom} and A_{aliph}, respectively, according to the following equation:

$$w_{PS,NMR} = \frac{M_S \times A_{arom}}{M_S \times A_{arom} + M_{IB}(5A_{aliph} - 3A_{arom})/8} \qquad (1)$$

M_S and M_{IB} represent the molecular weights of styrene and isobutylene repeat units, respectively. Spectra were obtained using a 300 MHz Bruker ACE-300 NMR spectrometer. Samples were analyzed as 5% (w/v) solutions in $CDCl_3$, and chemical shifts were determined relative to an internal reference (0 ppm) of tetramethylsilane (TMS). PS block molecular weight (M_{PS}) was calculated from $w_{PS,NMR}$ and the peak molecular weight of the PIB inner block ($M_{p,PIB}$) obtained by GPC:

$$M_{PS} = \frac{M_{p,PIB} \times w_{PS,NMR}}{2(1 - w_{PS,NMR})} \qquad (2)$$

the volume fraction PS (ϕ_{PS}) was calculated for each sample using the densities 1.05 and 0.92 g cm^{-3} for PS and PIB, respectively.

High resolution GPC (HRGPC) was performed using a Shell Development Co. proprietary system which employed a THF mobile phase at 50°C and dual refractive index (RI) and ultraviolet (UV) detectors. Molecular weights and molecular weight distributions (MWD) were referenced to PS standards.

2.2. Polymer sulfonation

The polystyrene blocks of the triblock copolymer were lightly sulfonated with acetyl sulfate in refluxing methylene chloride ($MeCl_2$) using a modification of the method described by Thaler [15]. A portion of the sulfonated polymer solution (5 wt% in toluene with 1–2% (v/v) *n*-hexanol as polar cosolvent) was then titrated to a thymol blue endpoint using 0.05 N ethanolic KOH or NaOH in order to determine the level of sulfonation. The remainder of the sample solution was then fully neutralized by adding the appropriate amount of a methanolic KOH or NaOH solution. A representative sulfonation procedure was as follows: Into a 1000 ml round bottom flask equipped with a magnetic stir bar and condenser were charged 30.56 g polymer (19.2 wt% PS by NMR, 5.64×10^{-2} mol styrene units) and 400 ml $MeCl_2$. The solution was stirred and warmed to reflux temperature. Into a 25 ml volumetric flask immersed in an ice bath were charged 20 ml $MeCl_2$, 1.09 g (0.01 mol) acetic anhydride and 0.206 ml (0.38 g of

95% solution, 3.7×10^{-3} mol) sulfuric acid. The contents of the flask were mixed thoroughly and then added slowly to the stirred polymer mixture. The reaction was allowed to proceed for 5 h at reflux before termination by the addition of 20 ml (0.5 mol) methanol.

The sulfonated polymer solution was freed of excess sulfonating reagents by precipitation into boiling, deionized water with vigorous stirring. The resulting crumbs were removed and placed in several changes of rapidly stirred fresh boiling water for approximately 20 min before being rinsed with methanol and dried in a 40°C vacuum oven overnight. The dried, acid-form ionomer was redissolved in $MeCl_2$, and the above precipitation, washing and drying procedures were repeated.

The degree of sulfonation was determined as follows: to a 125 ml Erlenmeyer flask equipped with a magnetic stir bar were charged 1.5 g of sulfonated block copolymer (dried to a constant weight), 30 ml toluene, 0.3–0.6 ml *n*-hexanol, and several drops of a methanolic thymol blue solution (0.05 wt%). The polymer solution was then titrated with 0.05 N KOH solution in ethanol. The latter was standardized against a 0.100 N solution of HCl immediately before use.

Preparative neutralizations were carried out by adding a stoichiometric amount of the desired counterion as an alcoholic solution to a solution of the sulfonated polymer as follows: to a 500 ml Erlenmeyer flask equipped with a magnetic stir bar were charged 18.27 g of sulfonated block copolymer (32.8 wt% PS, 3.4 mol% sulfonated, 1.96×10^{-3} mol sulfonic acid moieties), 350 ml toluene and $\approx$3 ml hexyl alcohol. The contents were stirred and the temperature was raised and maintained in the range 80–100°C. After complete dissolution of the polymer was achieved, 19.3 ml of 0.10 N KOH (1.93×10^{-3} mol) solution in methanol was added drop-wise to the solution.

2.3. Solution casting of films

The neutralized ionomer solution was precipitated into methanol, and the ionomer was dried to constant weight in an 80°C vacuum oven. The dried ionomer was redissolved for solution casting by placing an appropriate weight for the desired final film thickness into a glass jar equipped with a Teflon-lined lid, adding the amount of tetrachloroethylene (TCE) required for a 5 wt% solution, and placing the jar on a shaker for several hours or overnight. Depending on the ion content, the result was either an extremely viscous solution or a firm gel. *n*-Hexanol was then added drop-wise and shaking was allowed to continue for 1–2 h with periodic inspections. As the ideal amount of hexanol was neared, 2–10 vol%, depending on the ion content, and sufficient time for mixing was allowed, the viscosity of the entire sample became much lower. After several additional hours of mixing on the shaker, the solution was poured into a container for drying as described below for the block copolymer films.

Block copolymer films (0.8–1.5 mm thick) were cast in Teflon-lined aluminum pans (17.5 × 8 cm) from 5% (w/v) solutions in tetrachloroethylene and dried at 50°C for 7 days before being placed in a vacuum oven for further drying and annealing. Ionomer films were produced under identical conditions using solutions containing 2–10 vol% *n*-hexanol as a polar cosolvent. The film container was tightly covered with Al foil with several pinholes to slow solvent evaporation. Vacuum drying and annealing were carried out for 1 day at 60°C and then 3–5 days at 130–145°C.

2.4. Transmission electron microscopy

Bright-field TEM micrographs were produced using a Jeol 100CX with an accelerating voltage of 100 kV and a magnification of 30,600, 29,000, or 20,000 ×. Samples were prepared by microtoming 50 nm thick sections using a Reichert-Jung Ultracut E ultramicrotome equipped with the Reichert-Jung FC 4E cryosectioning system with a knife temperature of −110°C and a sample temperature of −80°C. The sections were stained for 2 min using the vapors of aqueous RuO_4.

2.5. Small angle X-ray scattering

SAXS data were collected at room temperature using a Rigaku small angle scattering goniometer (SASG) with Kratky collimation employing a 18 mm × 0.01 mm slit and a sample-to-detector distance of 26.5 cm. The SASG was used simply as a mount for the collimation, vacuum chamber, beam stop and detector, and did not move during data acquisition. This collimation approximated an infinitely long slit system, simplifying the slit desmearing procedure. A Braun OED 50M platinum wire position sensitive detector (PSD) was used, allowing the entire small angle range to be collected at once. Copper K_α radiation ($\lambda = 0.154$ nm) was generated by a Rigaku RU-H2R rotating anode X-ray generator operating at 48 kV and 200 mA, and was filtered by 0.015 mm nickel foil. Angular calibration was performed using a powdered calcium stearate sample. Measured scattering intensities were corrected for sample absorption, air scattering, and parasitic scattering by the Kratky camera. The absolute scattering intensity was calculated by comparison to a polyethylene standard that was calibrated to a Lupolen standard. The through-view geometry (film normal parallel to the propagation direction of the incident beam) was used for all samples. Data were obtained over a scattering vector (**h**) range of 0.07–6 nm^{-1} with a resolution of 0.02179 nm^{-1} ($\mathbf{h} = 4\pi \sin\theta/\lambda$, where θ is half the scattering angle).

Slit desmearing was accomplished using the method of Gerber et al. [16], which involves calculation of the radial correlation function directly from the smeared intensity. The former is then used to estimate the desmeared intensity. The radial correlation function is a probability function related to the electron density distribution throughout a sample [16,17] and is the inverse Fourier transform of the scattering intensity distribution. Prior to desmearing, the

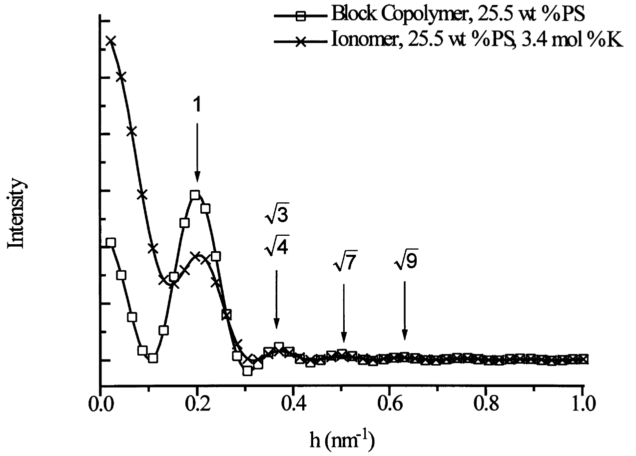

Fig. 1. Comparison of slit desmeared SAXS profiles for BCP01 and a corresponding ionomer containing 3.4 mol% potassium neutralized sulfonate groups.

smeared intensity at angles below the lowest measured angle was estimated by extrapolation [18], and additional background scattering arising from thermal fluctuations was subtracted from the measured intensity using Bonart's method [19].

3. Results and discussion

Sulfonated triblock copolymers were titrated at 80–100°C using a high boiling solvent such as toluene, xylenes, or tetrachloroethylene in conjunction with a high boiling cosolvent such as hexyl alcohol. This allowed precise control of solvent polarity throughout the titration by causing most of the added methanol to be boiled off. This is important because often the amount of added methanol results in precipitation of the sulfonated polymer, possibly preventing complete neutralization.

Films of PS–PIB–PS block copolymers and ionomers were carefully cast from dilute solution with the objective of achieving equilibrium or near-equilibrium morphologies. Toluene was considered for use as the casting solvent since it is often used for similar styrene–diene-based block copolymers and meets the general requirement of possessing a solubility parameter midway between those of the two constituent blocks. However, TCE was chosen for the present study as it produced superior films for tensile and dynamic mechanical analysis [20], and it was deemed important to perform morphological and mechanical properties investigations on the same films. The toluene-cast films exhibited irregular thickness and significant surface irregularities, such as depressions as large as 1 mm in diameter, despite careful control of the solvent evaporation rate. It was also desirable to use, as nearly as possible, the same solvent casting conditions for the block copolymers and the ionomers. The high boiling point (121°C) of TCE allowed very slow solvent evaporation at elevated temperatures which was found to be important when casting films of the ionomers.

Table 2
Observed vs. theoretical peak positions in SAXS analysis of PS–PIB–PS block copolymer samples (theoretical peak positions obtained by multiplying the scattering vector (**h**) of the first-order peak by the peak ratios characteristic of hexagonally packed cylinders (values at the top of each column))

Sample	ϕ_{PS}		1	$\sqrt{3}$	$\sqrt{4}$	$\sqrt{7}$	$\sqrt{9}$	$\sqrt{12}$
BCP04	0.172	Observed	0.23	0.39	0.51	**0.64**	**0.64**	0.76
		Theoretical	0.23	0.40	0.46	**0.61**	**0.69**	0.80
BCP01	0.231	Observed	0.20	**0.37**	**0.37**	0.50	0.63	0.75
		Theoretical	0.20	**0.35**	**0.40**	0.53	0.60	0.69
8907	0.296	Observed	0.22	0.38		0.51	0.63	0.76
		Theoretical	0.22	0.38	0.44	0.58	0.66	0.76
BCP02	0.308	Observed	0.20	**0.37**	**0.37**	0.50	0.63	0.76
		Theoretical	0.20	**0.35**	**0.40**	0.53	0.60	0.69

Casting films of the ionomers required the addition of a polar cosolvent to solvate the ionic domains. *n*-Hexanol was chosen to match the evaporation rate of the cosolvent with that of the primary solvent, preventing the gel formation that occurs when the cosolvent evaporates first. The required amount of polar cosolvent varied with degree of sulfonation, counterion type and trace amounts of residual water or other polar solvents remaining in the ionomer after purification procedures. Typical amounts used were 2–10 vol%, but a visual judgment of solution viscosity was necessary to determine the ideal amount for each sample. This procedure was found to produce films near their ideal or equilibrium morphology, as evidenced by identical DMA results before and after annealing at 225°C for 30 min and cooling slowly, over 2.5 h, to below 100°C. Films cast under non-ideal conditions, such as with too little polar cosolvent or one that evaporates too quickly, exhibited dramatic differences in dynamic mechanical properties before and after annealing [20].

Fig. 1 shows the slit desmeared SAXS profiles for samples BCP01 and an ionomer therefrom, which are typical of the materials in this study. The characteristic morphology of the discontinuous domains, i.e. whether spheres in a cubic lattice, cylinders in a hexagonal lattice, or lamellar, was determined from the scattering vector (**h**) values of higher order peaks relative to the first-order peak for interparticle scattering. Spheres arranged in a cubic lattice result in relative **h** values of $1, \sqrt{2}, \sqrt{3}, \sqrt{4}, \ldots$, cylinders arranged in a hexagonal lattice result in relative **h** values of $1, \sqrt{3}, \sqrt{4}, \sqrt{7}, \sqrt{9}, \sqrt{12}, \ldots$, and a lamellar morphology results in relative **h** values of 1, 2, 3, 4,… [8,9]. In all samples, including the ionomers, the peak maxima were found at ratios corresponding to those of hexagonally packed cylinders. Peaks at relative scattering vector ratios of $1, \sqrt{3}, \sqrt{4}, \sqrt{7}, \sqrt{9}$, and $\sqrt{12}$ correspond to d_{100}, d_{110}, d_{200}, d_{210}, d_{300} and d_{220}, respectively, where d_{hk0} is the lattice spacing of the ($hk0$) planes [21].

Table 2 lists the observed peak positions for each block copolymer sample followed by theoretical peak positions

Table 3
Morphological parameters calculated from SAXS data for PS–PIB–PS block copolymers

Sample	ϕ_{PS}	First-order **h** (nm^{-1})	d_{100} [a] (nm)	Interdomain distance,[b] a (nm)	Cylinder diameter (nm)
BCP04	0.172	0.23	27.3	31.5	13.7
BCP01	0.231	0.20	31.4	36.3	18.2
8907	0.296	0.22	28.6	33.0	18.8
BCP02	0.308	0.20	31.4	36.3	21.1
BCP01 Ionomer 3.4% K	0.231	0.21	29.9	34.5	17.4
8907 Ionomer 1.5% Na	0.296	0.28	22.4	25.9	14.8

[a] Bragg spacing, $d_{100} = 2\pi/\mathbf{h}$.

[b] Interdomain distance, $a = d_{100}\sqrt{4/3}$, for hexagonally packed cylinders.

obtained by multiplying the scattering vector (**h**) of the first-order peak by the ratio shown at the top of each column. In some cases, two peaks of consecutive order, e.g. the second- and third-order peaks for sample BCP01, apparently had sufficient overlap to produce only a single peak, whose position is listed in both columns (in bold typeface). In addition, individual peaks were occasionally missing, as for example the third-order peak in sample 8907, due to the convolution of interparticle and intraparticle scattering, and the effects of particle volume fraction on observed scattering profiles. A minimum in the SAXS profile, which would result solely from intraparticle scattering, often occurs very near a maximum in the SAXS profile due to interparticle scattering, resulting in one or more peaks being obscured. These effects, as well as those due to paracrystalline distortion, have been discussed in detail by Hashimoto et al. [21].

Bragg spacings and cylinder spacings (interdomain distances) were determined from the SAXS profiles and are listed in Table 3. The Bragg spacing, d_{100}, was obtained from the first-order peak position by $d_{100} = 2\pi/\mathbf{h}$; it was then related to the interdomain spacing or cell edge, a, for hexagonally packed cylinders (Fig. 2) by $a = d_{100}\sqrt{4/3}$. The interdomain spacing thus obtained represents the average distance between centers of cylinders. The cylinder spacings for all block copolymer samples were very similar as would be expected since all have very similar PIB inner-block molecular weights as shown in Table 1. The only anomaly was seen in the ionomer derived from sample 8907, but this sample had poorly developed phase morphology and is a good example of an ionomer cast under less than ideal conditions. This same sample exhibited dramatic changes in dynamic mechanical properties after one heating cycle from −120 to 320°C, with the second run having characteristics of properly cast, thoroughly annealed samples.

Peaks due to isolated particle scattering were not observed in the SAXS profiles; therefore cylinder diameters, d (Table 3) were calculated from space filling considerations, based on the geometry of hexagonally packed cylinders and the volume fraction of the minor phase, ϕ_{PS}, as determined from NMR [22]: $d = a\sqrt{(2\phi\mathrm{PS}\sqrt{3})/\pi}$. This equation is applicable only for hexagonally packed cylinders, but similar equations are available for spheres on a cubic lattice [9] or for lamellar [23] systems. For the block copolymers, cylinder diameters were observed to be reasonably proportional to $M_{PS}^{0.643}$, as predicted by Helfand and Wasserman [24] for block copolymers in the strong segregation limit. Cylinder diameters for BCP01 and its ionomer were essentially the same at 18.2 and 17.4 nm, respectively. The cylinder diameter for the ionomer derived from 8907 was much smaller than in the parent block copolymer and is indicative of the non-equilibrium morphology of this ionomer sample as described above.

Porod analysis was performed on the slit-smeared data using a protocol similar to Koberstein et al. [25]. Positive deviations from Porod's law were observed in plots of $\mathbf{h}^3 I$ vs. $\mathbf{h}^2$ for all samples (Fig. 3 is representative), indicating sharp phase boundaries and the possible presence of isolated phase mixing [17]. Diffuse phase boundaries would result in

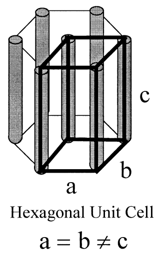

Fig. 2. Hexagonal unit cell (outlined in bold lines) showing lattice parameters *a*, *b* and *c*.

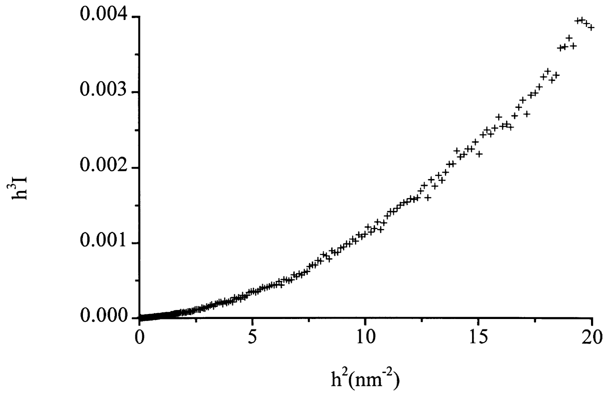

Fig. 3. Plot of $\mathbf{h}^3 I$ vs. $\mathbf{h}^2$ for BCP01 showing typical positive deviation from Porod's law.

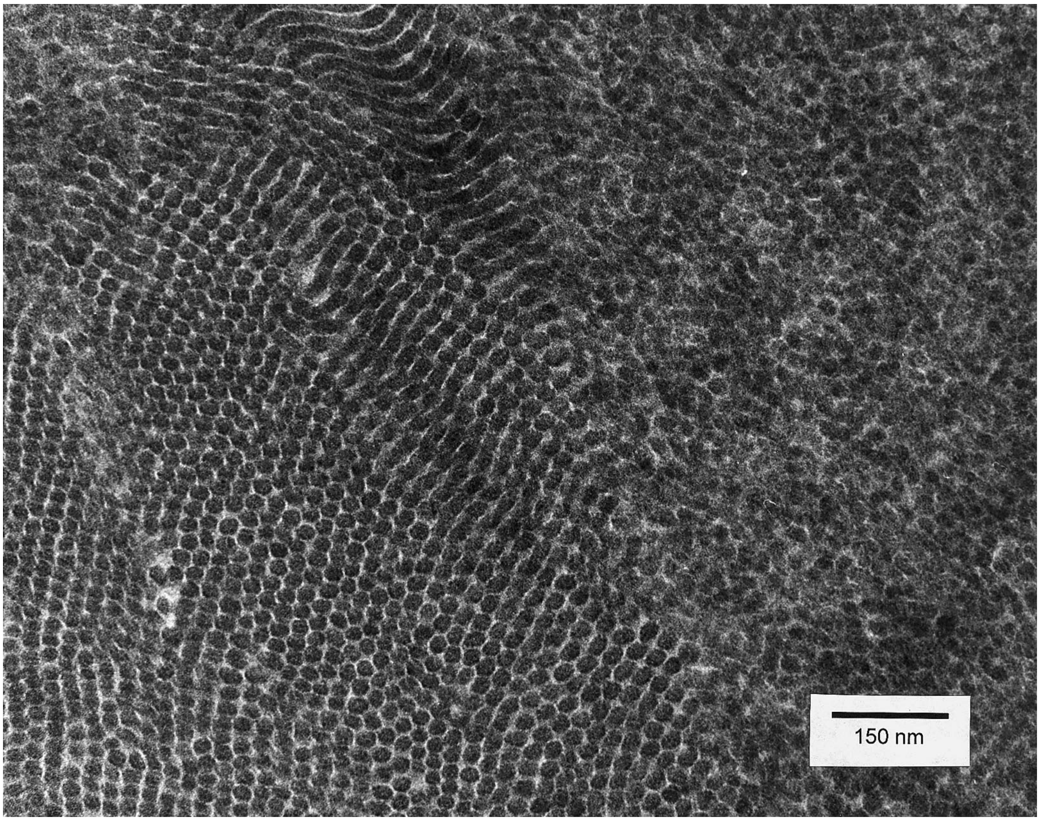

Fig. 4. TEM micrograph of phase-separated structure in BCP01 showing hexagonally packed cylinders of PS.

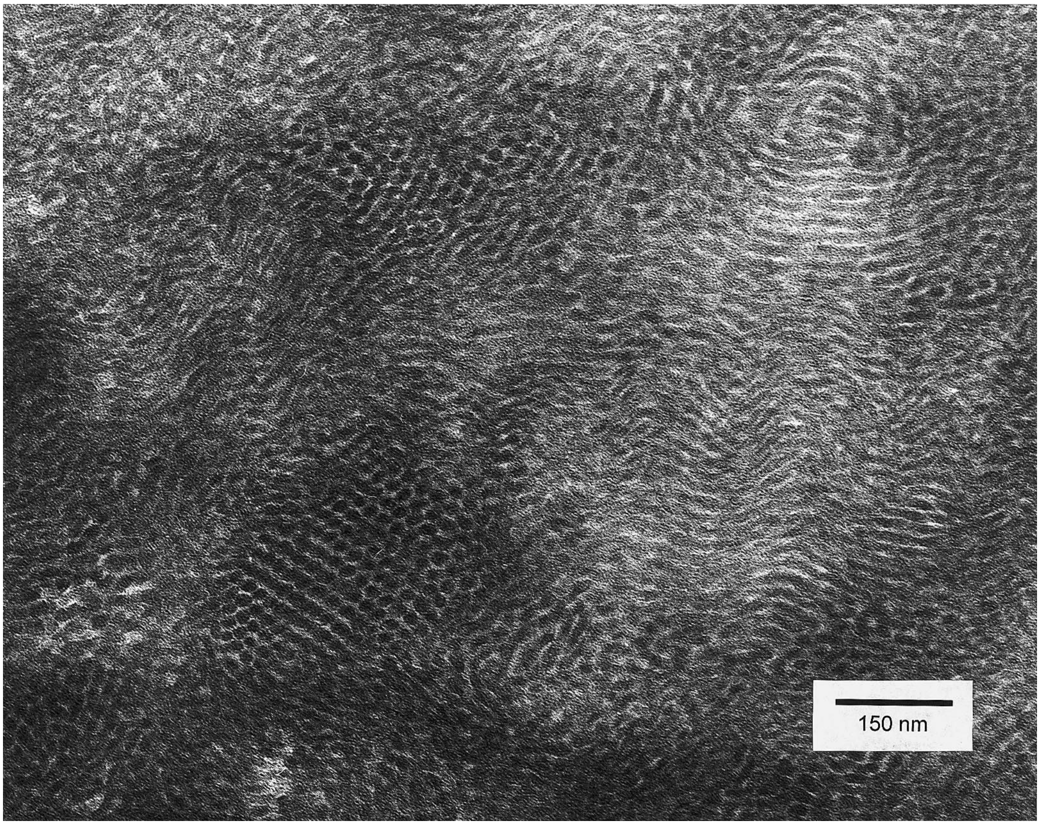

Fig. 5. TEM micrograph of phase-separated structure in BCP01 ionomer (3.4 mol% sulfonated, K counterion) showing hexagonally packed cylinders of PS ionomer.

negative deviations from Porod's law. This result is supported by the results of dynamic mechanical analysis that are presented in the third paper in this series [20].

Figs. 4 and 5 show the TEM micrographs of BCP01 and the ionomer derived therefrom, respectively. Fig. 4 is typical of the block copolymer samples, exhibiting a grain structure in which the cylinders within a given grain are aligned. In both micrographs, hexagonally packed cylindrical domains are seen, although there appears to be more order in the parent block copolymer, as one might expect due to the decreased mobility of the ionomer. In both samples, the cylinder spacing and diameter were similar, which is consistent with the SAXS results shown in Table 3.

4. Conclusions

SAXS and TEM data were presented for four PS–PIB–PS block copolymers with similar inner block molecular weights and PS volume fractions ranging from 0.17 to 0.31. All samples exhibited a phase-separated morphology consisting of hexagonally packed cylinders of PS dispersed within a PIB matrix. Cylinder spacing remained constant while cylinder diameters varied from 14 to 21 nm and were proportional to the square root of the PS block molecular weight. Sharp phase boundaries were indicated by Porod analysis. Also presented, for the first time, was a TEM micrograph clearly showing a hexagonally packed cylindrical PS ionomer phase within a block copolymer ionomer. The realization of such well-developed long-range order was primarily a result of very careful control of the solvent system and evaporation rate during film formation of these ionomers.

Acknowledgements

The research upon which this material is based was supported in part by the National Science Foundation through Grant No. EPS-9452857, and in part by the Army Research Office through Grant No. DAAH04-96-1-0191. The authors would also like to thank Dr Ed Rightor and the Dow Chemical Company for assistance with and use of their SAXS equipment, and Shell Development Co. for providing high resolution GPC.

References

[1] Kaszas G, Puskas JE, Kennedy JP, Hager WG. J Polym Sci, Polym Chem Ed 1991;29:427.
[2] Storey RF, Chisholm BJ. Macromolecules 1993;26:6727.
[3] Storey RF, Chisholm BJ, Choate KR. JMS—Pure Appl Chem 1994;A31(8):969.
[4] Storey RF, Chisholm BJ, Masse MA. Polymer 1996;37(14):2925.
[5] Gyor M, Fodor Z, Wang H-C, Faust R. JMS—Pure Appl Chem 1994;A31(12):2055.
[6] Fodor Z, Faust R. JMS—Pure Appl Chem 1996;A33(3):305.
[7] Storey RF, Chisholm BJ, Lee Y. Polym Engng Sci 1997;37(1):73.
[8] Sakurai S, Momii T, Taie K, Shibayama M, Nomura S, Hashimoto T. Macromolecules 1993;26:485.
[9] Sakurai S, Kawada H, Hashimoto T, Fetters LJ. Macromolecules 1993;26:5796.
[10] Lu X, Steckle WP, Weiss RA. Macromolecules 1993;26:6525.
[11] Weiss RA, Sen A, Pottick LA, Willis CL. Polym Commun 1990;31:220.
[12] Weiss RA, Sen A, Pottick LA, Willis CL. Polymer 1991;32(10):1867.
[13] Weiss RA, Sen A, Pottick LA, Willis CL. Polymer 1991;32(15):2785.
[14] Storey RF, Baugh DW, Choate KR. Polymer 1999;40:3083 Part II: this paper; Part III: Storey RF, Baugh DW. Poly(styrene-*b*-isobutylene-*b*-styrene) block copolymers produced by living cationic polymerization. III. Dynamic mechanical and tensile properties, in preparation.
[15] Thaler WA. J Polym Sci, Polym Chem Ed 1982;20:875.
[16] Gerber Th, Walter G, Kranold R. J Appl Crystallogr 1982;15:143.
[17] Tyagi D, McGrath JE, Wilkes GL. Polym Engng Sci 1986;26(20):1371.
[18] Heaney MD. PhD thesis, University of Colorado, 1988.
[19] Bonart R, Muller EH. J Macromol Sci Phys 1974;B10:177.
[20] Storey RF, Baugh DW. Poly(styrene-*b*-isobutylene-*b*-styrene) block copolymers produced by living cationic polymerization. III. Dynamic mechanical and tensile properties, in preparation.
[21] Hashimoto T, Kawamura T, Harada M, Tanaka H. Macromolecules 1994;27:3063.
[22] Morrison FA, Winter HH. Macromolecules 1989;22:3533.
[23] Tanaka H, Hasegawa H, Hashimoto T. Macromolecules 1991;24:240.
[24] Helfand E, Wasserman ZR. Macromolecules 1976;9:879.
[25] Koberstein JT, Morra B, Stein RS. J Appl Crystallogr 1980;13:34.